Journal of Power Sources 196 (2011) 6498–6501

Contents lists available at ScienceDirect

Journal of Power Sources

journal homepage: www.elsevier.com/locate/jpowsour

Short communication

Effect of copper doping on $LiMnPO_4$ prepared via hydrothermal route

Jiangfeng Ni, Lijun Gao*

School of Energy, Soochow University, Suzhou 215006, China

ARTICLE INFO

Article history:
Received 11 December 2010
Received in revised form 30 January 2011
Accepted 28 March 2011
Available online 6 April 2011

Keywords:
Lithium ion battery
Lithium manganese phosphate
Doping
Electrochemical activity

ABSTRACT

Fine-sized, well-crystallized $LiMnPO_4$ and two Cu-doped derivatives (2% and 5% Cu^{2+} doping) are readily prepared via a hydrothermal route. X-ray diffraction (XRD) combined with structural analysis, scanning electron microscopy (SEM), transmission electron microscopy (TEM), specific surface area analysis, and galvanostatic charge–discharge tests are applied to characterize these materials. The structure analysis shows that only a negligible amount of Cu^{2+} ions (0.2%) occupy the Li sites in the 2% Cu-doped material, while a considerable amount of Cu^{2+} ions (1.8%) occupy the Li sites in the 5% Cu-doped one. The electrochemical tests show that the 2% Cu-doped $LiMnPO_4$ displays an improved electrochemical performance compared with the undoped $LiMnPO_4$, while the 5% Cu-doped $LiMnPO_4$ exhibits a decreased activity.

1. Introduction

Recent applications of Li-ion batteries in large stationary power supplies and hybrid electric vehicles (HEVs) demand Li-ion batteries with higher energy density and improved safety. Due to intrinsically stable nature and favorable electrochemical properties, olivine $LiMPO_4$ (M = Fe, Mn, Co, Ni) materials have received a great deal of attention, since they were firstly proposed as cathode materials for Li-ion batteries by Padhi et al. in 1997 [1,2]. Over the last two decades, most interest was drawn to $LiFePO_4$, while little attention was paid to another member in this olivine family, $LiMnPO_4$ [3]. In fact, $LiMnPO_4$ seems more promising in performance than $LiFeO_4$ due to higher operating voltage (4.1 V vs. Li^+/Li), which contributes to a 20% increase in energy density [1]. However, due to poor electrochemical activity, the achievement of such high energy density remains a challenge [4,5]. Although occasionally Li et al. reported a high active $LiMnPO_4$ with a reversible capacity of ca. 140 mAh g^{-1} [3], such a good result has not been reproduced for a long period. Several factors are proposed to account for this issue, including low electronic and ionic conductivity, strong electron-lattice interaction (Jahn–Teller deformation), internal stress due to lattice misfit between $LiMnPO_4$ phase and $MnPO_4$ phase [4–7].

Recently, it is found that the electrochemical activity of $LiMnPO_4$ can be markedly improved when carefully controlling the size, morphology and texture of the material [8–11]. For example, Bakenov and Taniguchi [9] demonstrated that the $LiMnPO_4$ nanoparticles prepared at a relatively low temperature of 500 °C could deliver a high capacity about 150 mAh g^{-1}, reminiscent of Li et al.'s result [3]. Another case in point is that Wang et al. prepared a platelet-like $LiMnPO_4$ nanostructure with a thin [0 2 0] plane via a polyol method, which can deliver a high capacity of 159 mAh g^{-1} at 50 °C. The improved electrochemical performance is probably due to the special morphology. The thin [0 2 0] plane (~20 nm) not only facilitates the Li diffusion in solid bulk, but also provides a flexible structure towards lattice deformation and volume variation [12]. However, this polyol route is usually a multiple-step synthesis and need a large amount of organic solvent, thus it may be unsuitable for scale-up application.

Another strategy to improve the activity of $LiMnPO_4$ is through doping of exotic ions [13–16]. However, the mechanism of doping has not been well understood so far, as Chen et al. discovered that $LiMnPO_4$ doping with Mg^{2+}, Fe^{2+}, Ni^{2+}, and Cu^{2+} increased the electrochemical activity, whereas doping with Zn^{2+} decreased the activity [13]. Previous reports primarily attributed the doping effect to the modification of electronic conductivity and lattice compatibility, while failed to consider the exact occupying site of doping ions in lattice. We propose that the occupying sites of the exotic ions have a major effect on the electrochemical behavior of the olivine material, as Li ion diffusion in lattice proceeds along a one-dimensional channel [17,18].

In this work, we report the structure, morphology, and electrochemical activity of Cu-doped $LiMnPO_4$ material prepared via a hydrothermal synthesis route. These results are correlated and analyzed to shed light on the effect and mechanism of Cu-doping on $LiMnPO_4$ property.

2. Experimental

$LiMnPO_4$ and two Cu-doped derivatives were prepared by a hydrothermal route mediated by ascorbic acid as described pre-

* Corresponding author. Tel.: +86 512 69153197; fax: +86 512 67870271.
E-mail address: gaolijun@suda.edu.cn (L. Gao).

0378-7753/$ – see front matter © 2011 Elsevier B.V. All rights reserved.
doi:10.1016/j.jpowsour.2011.03.073

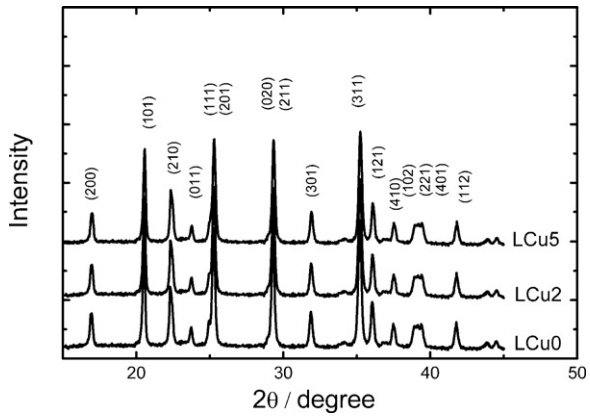

Fig. 1. XRD patterns of undoped $LiMnPO_4$ (LCu0) and two Cu-doped derivatives (LCu2 and LCu5) prepared via hydrothermal route.

viously [19]. In detail, a 30 mmol LiOH aqueous solution was mixed with 10 mmol H_3PO_4 at vigorous agitation. To this mixture a 10 mmol mixing Mn/Cu (Cu/(Cu + Mn) = 0, 0.02, 0.05) sulfate solution (accordingly the final products were denoted as LCu0, LCu2, and LCu5, respectively) was added drop-wise, followed by addition of 1.67 mmol ascorbic acid. The resultant suspension (~30 mL) was stirred for 10 min with Ar gas bubbling before it was transferred into a Teflon-lined stainless steel autoclave. The autoclave was further purged by Ar gas for five min, then sealed, and placed in an electric oven heated at 220 °C for 30 min. After reaction, the resultant light-gray precipitation was collected, washed by water and ethanol several times, and dried at 80 °C in vacuum. To improve conductivity, the obtained powder was coated with carbon by mixing with sucrose followed by heating at 600 °C for one hour. The total carbon content in the $LiMnPO_4$ materials was about 2.4 wt.%, as determined by measuring the weight loss of powders in air up to 600 °C.

X-ray diffraction (XRD) patterns of the materials were recorded using a Rigaku Dmax-2400 automatic diffractometer equipped with Cu K_α radiation (λ = 0.15406 nm). The diffraction data were collected from 15° to 100° employing a step scanning procedure at an interval of 0.02° with a count time of 2 s. The structural analysis was carried out with the Rietveld method on the program Rietan-2000 [20]. Scanning electron microscopy (SEM, JEOL JSM-6390) and transmission electron microscopies (TEM, JEOL JEM- 200CX) were performed to observe the morphology of the material particles. The specific surface area of $LiMnPO_4$ materials was measured on a ST08 Analyzer (Beifen Instrument, China) using the Brunauer, Emmett, and Teller (BET) method.

Electrochemical measurements were carried out using 2032 coin cells. The cathode composite consists of 80 wt.% active material, 10 wt.% acetylene black, and 10 wt.% polyvinylidene fluoride, with a typical material loading of 5 mg cm^{-2}. The 2032 coin cells were assembled in an Ar-filled glove box with a H_2O concentration below one ppm. The anode is Li metal foil, and the electrolyte is 1 mol L^{-1} $LiPF_6$ in ethylene carbonate/dimethyl carbonate (EC/DMC) (1:1 by volume). The cells were tested on a Land battery program-controlled test system in the voltage range of 2.2–4.5 V at 25 °C.

3. Results and discussion

The XRD patterns of three $LiMnPO_4$ materials (LCu0, LCu2, and LCu5) are presented in Fig. 1. All the patterns show well resolved diffraction peaks indexed to olivine $LiMnPO_4$ (JCPDS No. 74–0375) without any visible peaks due to impurities. In addition, the chemical composition of $LiMnPO_4$ materials is close to the expected formula, as determined by inductive coupled plasma (ICP) analysis. This indicates that the $LiMnPO_4$ materials were readily prepared via the ascorbic acid mediated hydrothermal process.

Table 1
The merit factors and structural parameters of as-prepared $LiMnPO_4$ materials.

Sample	S.G.	a (Å)	b (Å)	c (Å)	V (Å^3)	R_{wp} (%)	R_p (%)	S
LCu0	*Pnma*	10.442 (1)	6.098(1)	4.749(1)	302.43	3.45	2.76	1.88
LCu2	*Pnma*	10.440(1)	6.100(2)	4.742(1)	301.99	4.43	3.51	1.97
LCu5	*Pnma*	10.435(1)	6.096(3)	4.740(2)	301.52	4.32	3.26	1.74

Structural analysis based on the Rietveld refinement was performed on the XRD data. Some crystalline parameters were summarized in Table 1, and the refinement result of the typical sample of LCu2 is presented in Fig. 2. It is clearly seen that the observed pattern and calculated one fit well, implying that the refinement is reliable. The structural analysis of LCu0 reveals lattice parameters of a = 10.442(1) Å, b = 6.098(1) Å, c = 4.749(1) Å, and V = 302.43(4) Å^3, in good agreement with previous reports [4,14,18]. A slight decrease in lattice parameters is conformed for both Cu-doped materials, 301.99 Å^3 for LCu2 and 301.52 Å^3 for LCu5. This decrease in unit-cell volume proves the successful doping of Cu^{2+} in $LiMnPO_4$, as the doped cation (0.87 Å) has a smaller radius than Mn^{2+} ion (0.97 Å).

The Cu^{2+} ions were expected to substitute Mn. However, site occupation analysis shows that the Cu^{2+} ions occupy not only the Mn sites, but also the Li sites. Such disorder was confirmed by the merit factors of refinement. For instance, the merit factors R_{wp} and S decrease from 4.50% and 2.01 to 4.43% and 1.97, respectively, when allowing part Cu^{2+} ions disorder. About 0.2% Cu^{2+} ions occupy Li sites with 1.8% Cu^{2+} in Mn sites in LCu2, whereas in the case of LCu5, it is 1.8% and 3.2%, respectively. Although Cu^{2+} ions prefer to occupy the Mn sites, they may occupy the Li sites as well, due to the similar radius between Cu^{2+} (0.87 Å) and Li^+ (0.90 Å) [21]. Furthermore, such cation disorder would become remarkable when the reaction temperature [18] or time (in this case) is not enough to overcome the kinetic limitation and reach an ordered state. Since Li diffusion in $LiMnPO_4$ through the one-dimensional channel, a considerable amount of Cu^{2+} ions in Li sites will exert an adverse effect on Li diffusion.

Fig. 3a–c illustrates the SEM images of three $LiMnPO_4$ materials before carbon coating. All materials are composed of fine particles, and a low concentration doing of Cu does not change the size and morphology of $LiMnPO_4$. As discussed before, ascorbic acid molecules can effectively mediate the crystallization process of phosphate under the hydrothermal conditions, leading to fine sized particles and uniform size distribution [19]. Fig. 3d shows a TEM image of the typical LCu2 material after carbon coating. It

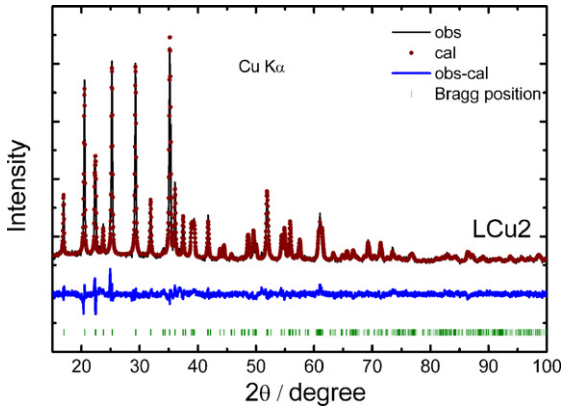

Fig. 2. Rietveld refinement results of the 2% Cu-doped $LiMnPO_4$ material.

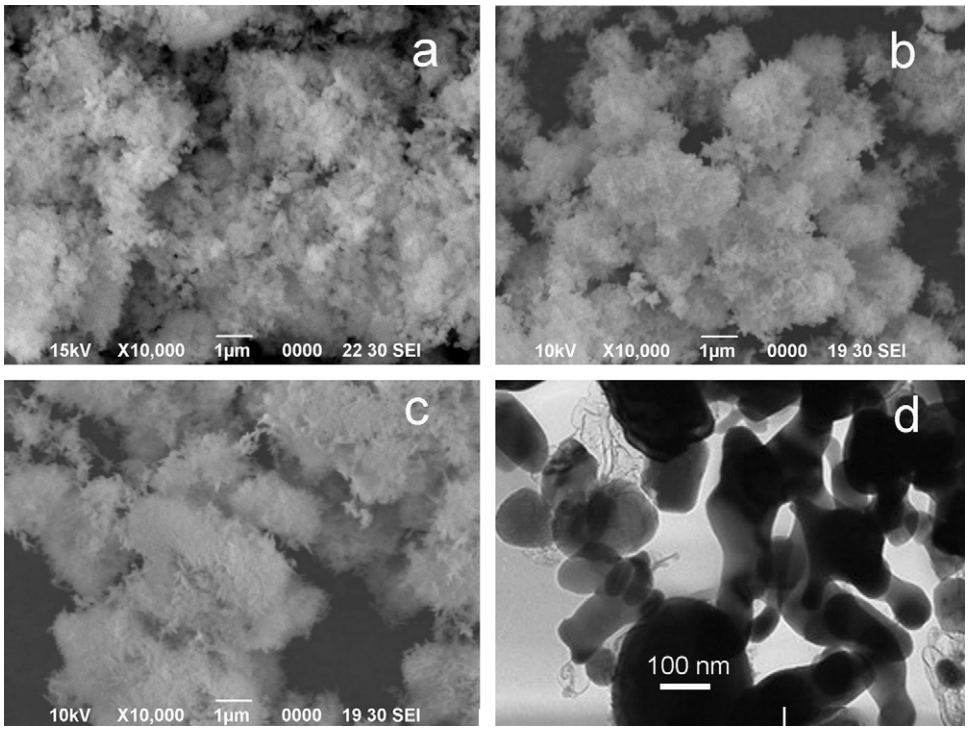

Fig. 3. SEM images of (a) LCu0, (b) LCu2, and (c) LCu5. (d) TEM image of LCu2.

reveals that most particles are about 100 nm, and they are interconnected by carbon. The three samples show close specific surface areas: 16.9, 17.8, 17.9 $m^2\ g^{-1}$ for LCu0, LCu2, and LCu5, respectively, as determined by N_2 absorption. This is easy to understand since the samples were prepared under nearly the identical condition.

Fig. 4a compares the initial charge and discharge profiles of the three materials at 0.1 C (1 C = 150 mA g^{-1}) at 25 °C. All the materials display a flat plateau around 4.0 V, indicating a two-phase ($LiMnPO_4 \leftrightarrow MnPO_4$) transformation process. In the range of 2.2–4.5 V, LCu0 delivers a capacity of 101 mAh g^{-1}, whereas LCu2 shows an increased capacity of 121 mAh g^{-1} and LCu5 exhibits a decreased capacity of 76 mAh g^{-1}. Since all the materials show similar surface areas and have the same carbon coating content, the difference in the electrochemical activity is primarily attributed to the total conductivity, which is proportional to both electronic and ionic conductivity in parallel [22]. On one hand, Cu^{2+} doping can bring about new impurity energy levels in the forbidden band, and thus increase the electronic conductivity [16]. On the other hand, dopant Cu^{2+} in Li site may block the one-dimensional diffusion channel, leading to a degraded ionic conductivity [18]. Therefore, the effect of doped cation on the total conductivity will depend on which one is dominant. In the case of LCu2, only 0.2% Cu^{2+} ions occupy Li sites and their influence on Li diffusion is negligible. In the case of LCu5, however, 1.8% Cu^{2+} ions occupying Li sites significantly impede the transportation of Li. As a result, LCu2 shows an increased total conductivity as well as activity compared with LCu0 while LCu5 exhibits a decreased one. It is worth mentioning that our results are consistent with that of Monte Carlo simulation on $LiFePO_4$ [17]. Compared with previous reports on ion-doped $LiMnPO_4$, the capacity of LCu2 is close to the result reported by Lee et al. [15], while somewhat lower than that by Shiratsuchi et al. [14], probably due to the low carbon contents in electrodes in Lee's and our cases (9.5–12 wt.% compared with 25 wt.%). This is indeed the case as recent research works manifest that the performance of $LiMnPO_4$ largely relies on the amount and nature of coating carbon [23,24]. The cycling behaviors presented in Fig. 4b show a similar correlation. The LCu2 sample exhibits the highest capacity retention of 94% after 20 cycles, while LCu0 and LCu5 only remain 89% and 86% of their initial values, respectively.

To better understand the effect of Cu doping on the activity of $LiMnPO_4$, the differential curves (dQ/dV) derived from charge

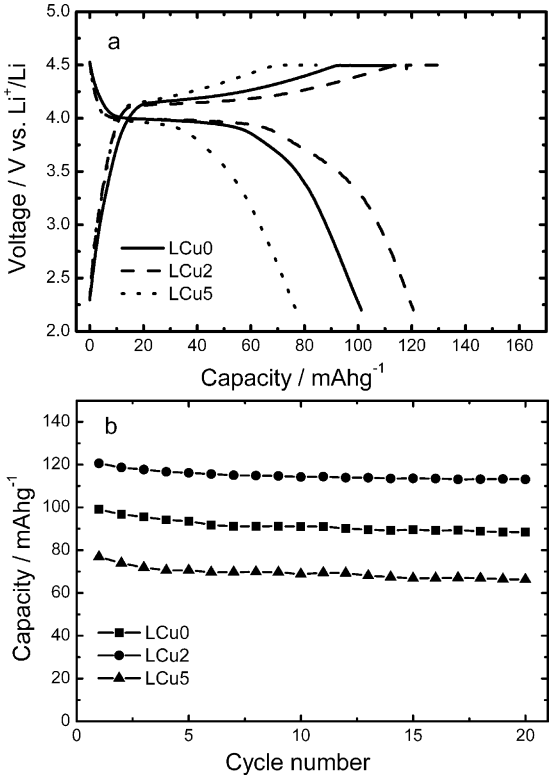

Fig. 4. (a) The initial charge and discharge profiles of three $LiMnPO_4$ materials at 0.1 C. The cells are charged at a CC-CV protocol, i.e., first charged at a constant current of 0.1 C to 4.5 V followed by holding at 4.5 V until current decaying to 0.02 C. (b) The discharge capacity at 0.1 C as a function of the cycle number.

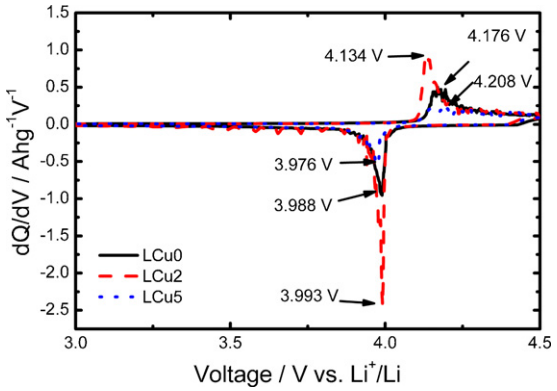

Fig. 5. The differential curves (d*Q*/d*V*) corresponding to Fig. 4a.

and discharge profiles (Fig. 4a) are given in Fig. 5. Regarding the d*Q*/d*V* curves, the intensity of anodic and cathodic peaks and their potential interval are two important parameters determining the electrochemical property. The high peak intensity and small potential interval are characteristic of good electrochemical performance. It is seen that the peak intensity increases in the sequence of LCu5 < LCu0 < LCu2, while the potential interval shows an opposite order, 0.131, 0.188 and 0.232 V for LCu2, LCu0 and LCu5, respectively. This clearly verifies that the electrochemical activity is improved in LCu2, while it is decreased in LCu5.

4. Conclusion

In summary, well-crystallized $LiMnPO_4$ and two Cu-doped derivatives were prepared via a modified hydrothermal route. Structural analysis shows that there are only 0.2% Cu^{2+} ions occupying Li sites in 2% Cu-doped $LiMnPO_4$, whereas 1.8% Cu^{2+} ions in Li sites in 5% Cu-doped $LiMnPO_4$. Although Cu-doping has a positive effect on the electronic conductivity, it may block the Li diffusion pathway if Cu^{2+} ions occupy the Li site. As a result, 2% Cu-doped $LiMnPO_4$ shows an increased electrochemical activity, whereas 5% Cu-doped material exhibits a decreased one. It should be noted that this work has only examined the divalent Cu^{2+} ion doping. Doping with other supervalent ions may have varied results [25,26]. The results clearly demonstrate that site occupation is an important factor influencing the doping effect of olivine materials.

References

[1] A.K. Padhi, K.S. Nanjundaswamy, J.B. Goodenough, J. Electrochem. Soc. 144 (1997) 1188–1194.
[2] A.K. Padhi, K.S. Nanjundaswamy, C. Masquelier, S. Okada, J.B. Goodenough, J. Electrochem. Soc. 144 (1997) 1609.
[3] G.H. Li, H. Azuma, M. Tohda, Electrochem. Solid-State Lett. 5 (2002) A135.
[4] S. Okada, S. Sawa, M. Egashira, J.-I. Yamaki, M. Tabuchi, H. Kageyama, T. Konishi, A. Yoshino, J. Power Sources 97–98 (2001) 430.
[5] A. Yamada, M. Hosoya, S.-C. Chung, Y. Kudo, K. Hinokuma, K.-Y. Liu, Y. Nishi, J. Power Sources 119–121 (2003) 232.
[6] Z.X. Nie, C.Y. Ouyang, J.Z. Chen, Z.Y. Zhong, Y.L. Du, D.S. Liu, S.Q. Shi, M.S. Lei, Solid State Commun. 150 (2010) 40.
[7] C. Delacourt, P. Poizot, M. Morcrette, J.-M. Tarascon, C. Masqulier, Chem. Mater. 19 (2004) 93.
[8] N.-H. Kwon, T. Drezen, I. Exnar, I. Teerlinck, M. Isono, M. Graetzel, Electrochem. Solid-State Lett. 9 (2006) A277.
[9] Z. Bakenov, I. Taniguchi, Electrochem. Commun. 12 (2010) 75–78.
[10] S.K. Martha, B. Markovsky, J. Grinblat, Y. Gofer, O. Haik, E. Zinigrad, D. Arubach, T. Drezen, D. Wang, G. Deghenghi, I. Exnar, J. Electrochem. Soc. 157 (2009) A541.
[11] D. Wang, H. Buqa, M. Crouzet, G. Deghenghi, T. Drezen, I. Exnar, N.-H. Kwon, J.H. Miners, L. Poletto, M. Gratzel, J. Power Sources 189 (2009) 624.
[12] Y.-G. Guo, J.-S. Hu, L.-J. Wan, Adv. Mater. 20 (2008) 2878.
[13] G. Chen, J.D. Wilcox, T.J. Richardson, Electrochem. Solid-State Lett. 11 (2008) A190.
[14] T. Shiratsuchi, S. Okada, T. Doi, J. Yamaki, Electrochim. Acta 54 (2009) 3145.
[15] J.-W. Lee, M.-S. Park, B. Anass, J.-H. Park, M.-S. Paik, S.-G. Doo, Electrochim. Acta 55 (2010) 4162.
[16] D. Wang, C. Ouyang, T. Drézen, I. Exnar, A. Kay, N.-H. Kwon, P. Gouerec, J.H. Miners, M. Wang, M. Grätzel, J. Electrochem. Soc. 157 (2010) A225.
[17] C.Y. Ouyang, S.Q. Shi, Z.X. Wang, H. Li, X.J. Huang, L.Q. Chen, J. Phys.: Condens. Matter 16 (2004) 2265.
[18] H. Fang, Z. Pan, L. Li, Y. Yang, G. Yan, G. Li, S. Wei, Electrochem. Commun. 10 (2008) 1071.
[19] J. Ni, M. Morishita, K. Yoshiteru, M. Watada, N. Takeichi, T. Sakai, J. Power Sources 195 (2010) 2877.
[20] F. Izumi, T. Ikeda, Mater. Sci. Forum (2000) 321.
[21] R.D. Shannon, Acta Crystallogr. A32 (1976) 751.
[22] C. Wang, J. Hong, Electrochem. Solid-State Lett. 10 (2007) A65.
[23] S.-M. Oh, S.-W. Oh, C.-S. Yoon, B. Scrosati, K. Amine, Y.-K. Sun, Adv. Funct. Mater. 20 (2010) 3260.
[24] Z. Bakenov, I. Taniguchi, J. Power Sources 195 (2010) 7445.
[25] M.S. Islam, D.J. Driscoll, C.A.J. Fisher, P.R. Slater, Chem. Mater. 17 (2005) 5085.
[26] M. Wagemaker, B.L. Ellis, D. Lützenkirchen-Hecht, F.M. Mulder, L.F. Nazar, Chem. Mater. 20 (2008) 6313.